Internal Rogue Waves in Stratified Flows and the Dynamics of Wave Packets

T. Y. Liu*, H. N. Chan*, R. H. J. Grimshaw†, K. W. Chow*‖

* = Department of Mechanical Engineering,

University of Hong Kong, Pokfulam, Hong Kong

† = Department of Mathematics, University College London,

Gower Street, London WC1E 6BT, United Kingdom

‖ = Corresponding author

Phone: (852) 3917 2641 Fax: (852) 2858 5415 Email: kwchow@hku.hk

Submission date: March 2018

PACS: 47.35.-i, 47.55.Hd, 47.35.Fg

Declaration of interest: None

ABSTRACT

A theoretical study on the occurrence of internal rogue waves in density stratified flows is conducted. While internal rogue waves for long wave models have been studied in the literature, the focus here is on unexpectedly large amplitude displacements arising from the propagation of slowly varying wave packets. In the first stage of the analysis we calculate new exact solutions of the linear modal equations in a finite domain for realistic stratification profiles. These exact solutions are then used to facilitate the calculations of the second harmonic and the induced mean motion, leading to a nonlinear Schrödinger equation for the evolution of a wave packet. The dispersion and nonlinear coefficients then determine the likelihood for the occurrence of rogue waves. Several cases of buoyancy frequency (N) are investigated. For N^2 profiles of hyperbolic secant form, rogue waves are unlikely to occur as the dispersion and nonlinear coefficients are of opposite signs. For N^2 taking constant values, rogue waves will arise for reasonably small carrier envelope wavenumbers, in sharp contrast with the situation for a free surface, where the condition is $kh > 1.363$ (k = wavenumber of the carrier envelope, h = depth). Finally, a special N^2 profile permits an analytical treatment for a linear shear current. Unexpectedly large amplitude waves are possible as the dispersion and nonlinear coefficients can then be of the same sign.

Keywords: Stratified flows; Schrödinger systems; Rogue waves

1. Introduction

Stratified flows and internal waves occur frequently in the atmosphere and the oceans [1,2]. The dynamics and properties of such flows play an essential role in processes such as transport, mixing and the movement of nutrients in the oceans. Studies of small amplitude disturbances in stratified flows will then enhance the analytical description of the fluid motion, and have developed into a branch of classical hydrodynamic theory [3]. Concerning the dynamics of the oceans, a commonly used assumption is to employ the Boussinesq approximation, where the variation in the density is ignored except in the buoyancy term. In this approximation the governing equation for small disturbances is defined as an eigenvalue problem for the phase speed:

$$\left(U-c\right)\left(\phi_{yy}-k^2\phi\right)-U_{yy}\phi+\frac{N^2\phi}{U-c}=0, \tag{1}$$

where ϕ, $U = U(y)$, k, c are the modal function of the linearized vertical velocity field, background shear, wavenumber and wave speed respectively, and y is the vertical coordinate. N is the buoyancy frequency given by

$$N^2=-\frac{g}{\overline{\rho}}\frac{d\overline{\rho}}{dy} \quad (g \text{ is gravity}), \tag{2}$$

where $\overline{\rho}$ is the mean density profile in the undisturbed state. Extensive studies have been performed on this classical equation, ranging from special exact solutions [4] to stability considerations [5].

For the special case where a background shear flow is absent ($U(y) = 0$), this eigenvalue problem becomes the modal equation

$$\phi_{yy} + \left[\frac{N^2}{c^2} - k^2 \right] \phi = 0 , \qquad (3)$$

which, together with the boundary conditions, defines an eigenvalue problem for the speed c with a given input wavenumber k. For stable stratification, there is no instability in the absence of a current. In developing the theory for the propagation of waves with a modal function given by Eq. (3), it is necessary to determine the dispersion relation $\omega = \omega(k)$ where ω is the wave frequency, the group velocity

$c_g = \partial\omega/\partial k$,

and frequently $c_{gk} = \partial^2\omega/\partial k^2$ as well. For this purpose, it is useful if explicit solutions of Eq. (3) can be found. One objective of this work is to establish exact solutions for this reduced form of the eigenvalue problem Eq. (3), in particular for a special class of density profiles, namely, the buoyancy frequency being the square of the hyperbolic secant with respect to the vertical coordinate. The underlying methodology is to note a connection with the nonlinear Schrödinger equation (NLSE) from the theory of solitons. Special solutions from the NLSE theory are then employed in solving the eigenvalue problem Eq. (3). While knowledge from classical linear differential equations, e.g. Pöschl–Teller and reflectionless potentials [6], hypergeometric and Legendre functions, could be invoked for this 'sech square' profile, utilizing coupled Schrödinger models can generate eventually solutions for more complicated, and even asymmetric, density profiles.

To describe waves with larger amplitude, a Hamiltonian formulation or higher order perturbation scheme will be necessary. A Hamiltonian approach of a two-layer fluid with nonzero mean flow can demonstrate the properties of wave-current interactions vividly [7]. Investigations of higher order series expansion, e.g. the Witting series and the Karabut system, can also be utilized to elucidate solitary waves for fluids of a finite depth [8]. Indeed ingenious mathematical methodologies have been applied to reveal intriguing nonlinear dynamics of these hydrodynamic systems, e.g. an implicit function approach is employed for the propagation of capillary-gravity waves in a spherical coordinate system [9].

Similar to the case of surface waves, the propagation of weakly nonlinear internal wave trains in a continuously stratified fluid is described by the NLSE [10]. Among various solutions of the NLSE which are physically relevant to water waves, the Peregrine breather (PB) solution [11] has attracted substantial attention recently due to its application to model rogue waves in the ocean [12]. The localized nature of the PB in both space and time resembles the character of a rogue wave as an entity which ‘appears from nowhere and disappears without a trace’. Remarkably, PB and its higher order variations are realizable in water wave tanks [13,14]. In the context of surface waves, PB exists only in the focusing or deep water regime, i.e., the regime of $kh > 1.363$ (where k is the wavenumber of the carrier envelope and h is the depth) [15,16]. Indeed elegant mathematical techniques have been applied to find analytical expressions for rogue waves for other nonlinear evolution systems, e.g. Mel’nikov, Sasa-Satsuma and Fokas-

Lenells equations [17,18,19]. The objective here is to study the corresponding existence criterion of internal rogue waves in a stratified fluid.

The main results and the structure of this paper can now be explained. Starting from the traveling waves of coupled NLSEs [20–23], an exact solution of Eq. (3) for linear modes without background shear is derived for a density profile which resembles a pycnocline in the ocean. On utilizing formulation of systems of four and five coupled NLSEs [22,23], solutions with increasing complexity in terms of the vertical structures are established for flows in a finite channel (Section 2). The group velocity and the second derivative of the dispersion relation of these wave packets are derived analytically too (Section 3). The occurrence of internal rogue waves in a channel with or without background shear is then examined (Section 4). A further example with constant buoyancy frequency is studied in Section 5. Concluding remarks will be presented in Section 6.

2. Exact solutions of the linear modal problem in a finite channel

For a system consisting of multiple or P (P = positive integer) wave packets, the evolution of weakly nonlinear, weakly dispersive, complex valued envelopes (A_p, p = 1, 2…P) in many physical applications is governed by the coupled nonlinear Schrödinger equations [3, 20–24] (σ is a real parameter):

$$i\frac{\partial A_n}{\partial t}+\frac{\partial^2 A_n}{\partial x^2}+\sigma\left(\sum_{p=1}^{P}\left|A_p\right|^2\right)A_n=0,\quad n=1,2,\ldots P. \tag{4}$$

On looking for time harmonic oscillations

$$A_n = \psi_n(x)\exp(-i\Omega_n t), \tag{5}$$

where $\psi_n(x)$ is real-valued, the reduced form is

$$\frac{d^2\psi_n}{dx^2} + \left(\Omega_n + \sum_{p=1}^{P} \psi_p^2 \right) \psi_n = 0, \qquad n = 1, 2, \ldots P. \tag{6}$$

Periodic solutions with multiple peaks per period can be derived [20–23]. However, a surprising and remarkable feature is that the sum of the intensities ($\sum_{p=1}^{P} \psi_p^2$) in Eq. (6), or the total induced mean flow in the context of hydrodynamic waves, can be expressed in terms of the square of the hyperbolic secant. On comparing Eq. (6) and Eq. (3), one can deduce that the coupled nonlinear Schrödinger model can be applied to the stratified flow problem provided that the buoyancy frequency can also be expressed in terms of hyperbolic functions.

More precisely, we shall first consider a stratification profile in the form of the square of a hyperbolic secant:

$$N^2 = \alpha_1 \operatorname{sech}^2(ry) + \alpha_0, \text{ with constants } r,\ \alpha_1,\ \alpha_0 > 0. \tag{7}$$

The three parameters r, α_1, α_0 will be the input/starting point and in terms of fluid dynamics, they measure respectively the width of the pycnocline, the density jump and the far field density from the viewpoint of internal waves modeling.

To illustrate how the theory of nonlinear waves can be used, consider a concrete example with an elementary solution from the literature of the coupled nonlinear Schrödinger model Eq. (6),

$$\phi = \mathrm{sech}^2(ry) - \frac{2}{3}, \tag{8}$$

where we use the symbol ϕ for the convenience in subsequent presentations. This functional form will satisfy the linear modal problem Eq. (3) for the density profile Eq. (7) for a special wavenumber k and the associated wave speed c given by

$$k^2 = 6r^2 \frac{\alpha_0}{\alpha_1}, \quad c^2 = \frac{\alpha_0}{k^2}. \tag{9}$$

The actual background density can be readily computed from Eq. (2) and Eq. (7). The fluid will be stably stratified provided the parameters α_0, α_1 are positive. Figure 1 shows the buoyancy frequency N and the mean density profile $\overline{\rho}$ for typical values of the input parameters ($-H < y < H$, $r = 0.658$, $H = 1$, $\alpha_0 = \alpha_1 = 1$, density being unity at $y = 0$).

a

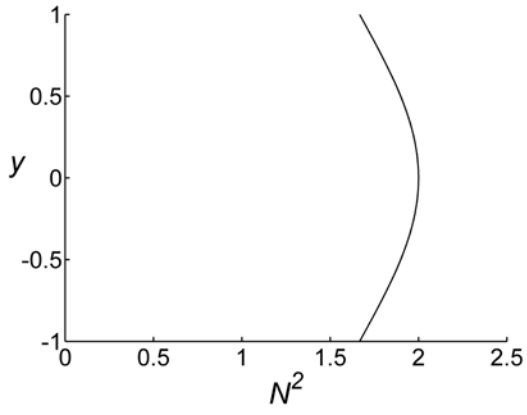

b

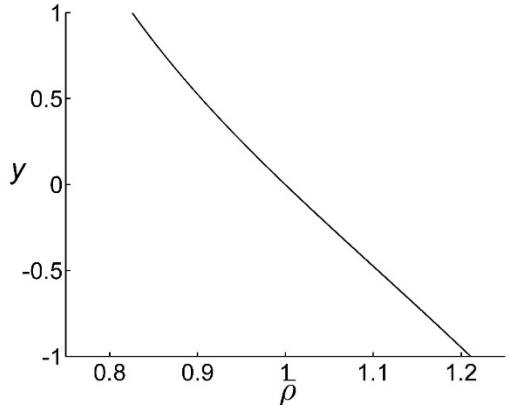

Fig. 1. (a) Plot of N^2 as a function of the vertical coordinate y, $-H < y < H$, $r = 0.658$, $\alpha_0 = \alpha_1 = 1$, $H = 1$. (b) Plot of the mean density profile $\overline{\rho}$ as a function of the vertical coordinate y, $-H < y < H$, $r = 0.658$, $\alpha_0 = \alpha_1 = 1$, $H = 1$.

2.1 Four coupled Schrödinger equations

Based on the solutions for a system of four coupled NLSEs [22,23], two of them will satisfy the boundary conditions of a finite channel with rigid boundaries, namely, $\phi(-H) = \phi(H) = 0$. The other solutions are valid for an infinite domain and will not be discussed in this paper. The first family of solutions of the linear modal problem Eq. (3) generated from four coupled nonlinear Schrödinger equations will thus be:

$$\phi_a = \operatorname{sech}(r_a y)\tanh(r_a y)\left[\operatorname{sech}^2(r_a y) - \frac{4}{7}\right], \tag{10}$$

$$k_a^2 = r_a^2\left(20\frac{\alpha_0}{\alpha_1} + 1\right), c_a^2 = \frac{\alpha_0}{k_a^2 - r_a^2}, \tag{11}$$

$$r_a = \frac{1}{H}\operatorname{sech}^{-1}\sqrt{\frac{4}{7}}\,. \tag{12}$$

The special value for r_a is calculated from the boundary condition where the eigenfunction ϕ_a must vanish at the rigid walls located at $y = \pm H$ (Fig. 2).

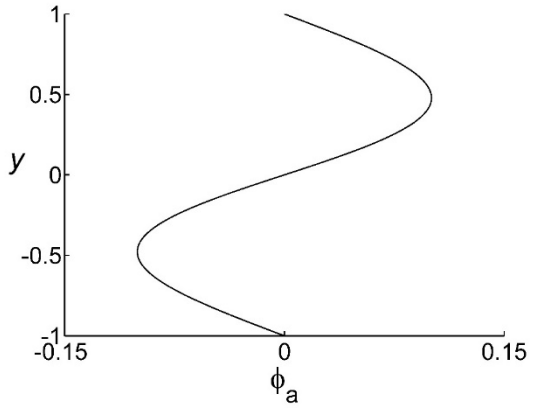

Fig. 2 The eigenfunction ϕ_a , Eq. (10), as a function of the vertical coordinate y, $-H < y < H$, $H = 1$, with r_a given by Eq. (12).

2.2 Five coupled Schrödinger equations

Based on a system of five coupled Schrödinger equations [23], five exact solutions of the linear modal problem Eq. (3) will be further identified where only three of them will satisfy the boundary conditions of a finite channel. We focus on the odd eigenfunction:

$$\phi_b = \operatorname{sech}^2(r_b y)\tanh(r_b y)\left[\operatorname{sech}^2(r_b y) - \frac{2}{3}\right], \tag{13}$$

$$k_b^2 = r_b^2\left(30\frac{\alpha_0}{\alpha_1} + 4\right), \quad c_b^2 = \frac{\alpha_0}{k_b^2 - 4r_b^2}, \tag{14}$$

$$r_b = \frac{1}{H}\operatorname{sech}^{-1}\sqrt{\frac{2}{3}}\ . \tag{15}$$

This eigenfunction must vanish at rigid walls located at $y = \pm H$ (Fig. 3). Eigenfunctions with more interior nodes can be found. Moreover, two other solutions with no finite zeros are possible. They are valid for fluids in unbounded domain and will not be discussed further in this paper.

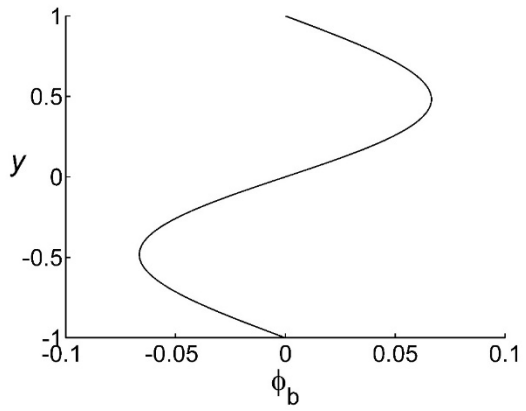

Fig. 3 The eigenfunction ϕ_b , Eq. (13), as a function of the vertical coordinate y, $-H < y < H$, $H = 1$, with r_b given by Eq. (15).

2.3 Numerical solutions of the linear modal equation for arbitrary wavenumber k

The exact solutions just tabulated are valid for special values of k (wavenumber) and r (stratification parameter). Numerical solutions of Eq. (3) would be necessary for arbitrary values of k and r. As an illustrative example, we consider the analytical solution for $k = 3.590$, $c = 0.284$, corresponding to $H = 1$, $\alpha_1 = 1$, $\alpha_0 = 1$ of Eqs. (10) through (12). The phase speed c for other values of k can be obtained by solving Eq. (3) numerically (Fig. 4). In general c will vary smoothly as a function of k, with the analytic solution picking out a few particular values of k.

We believe that the existence of analytical solutions will enhance our understanding of the fluid dynamics and will facilitate the development of nonlinear evolution of the wave trains. Furthermore, these settings of propagating internal waves also contrast sharply with certain scenarios in the stability of shear flows, where special analytic solutions have no other counterparts in the vicinity of that particular parameter regime.

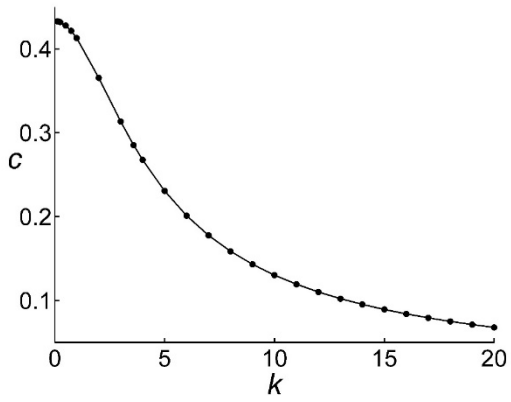

Fig. 4 A plot of the phase speed c versus the wavenumber k for a continuous range of k beyond the special analytical solution of $k = 3.590$, $c = 0.284$ for Eqs. (10-12), where the remaining data points are obtained by solving Eq. (3) numerically.

3. Group velocity

The analytic solutions described in Section 2 are valid for a specific fixed wavenumber k and angular frequency ω (or speed c). However, in applications we often need to find also the group velocity $c_g = \partial\omega/\partial k$, and usually $c_{gk} = \partial^2\omega/\partial k^2$ as well [24]. Since those two quantities are not available directly for these special solutions, we describe here how such information may be obtained, given only the knowledge of the

eigenfunction and the associated speed at this specific wavenumber. The modal equation Eq. (3) and boundary value problem are

$$\phi_{yy} + k^2\left[\frac{N^2}{\omega^2} - 1\right]\phi = 0, \quad -H < y < H, \quad \phi = 0 \text{ at } y = \pm H .$$

Multiply by ϕ and integrate by parts,

$$D(\omega, k) \equiv \int_{-H}^{H} \phi_y^2 dy - \int_{-H}^{H} k^2\left[\frac{N^2}{\omega^2} - 1\right]\phi^2 dy = 0.$$

This defines the dispersion relation $\omega = \omega(k)$ and also $\phi = \phi(y, k)$. Noting that we can regard ω as a "free variable", differentiation with respect to *k* then yields

$$D_\omega c_g + D_k = 0,$$

$$D_\omega = \int_{-H}^{H} 2k^2 \frac{N^2}{\omega^3}\phi^2 dy,$$

$$D_k = -\int_{-H}^{H} 2k\left[\frac{N^2}{\omega^2} - 1\right]\phi^2 dy .$$

The terms in D_k given by

$$\int_{-H}^{H} 2\phi_y \phi_{yk} dy - \int_{-H}^{H} k^2\left[\frac{N^2}{\omega^2} - 1\right] 2\phi\phi_k dy = 0,$$

vanish after integrating by parts. Differentiating again with respect to *k* will yield

$$D_\omega c_{gk} + D_{\omega\omega} c_g^2 + \left(D_{\omega k} + D_{k\omega}\right) c_g + D_{kk} = 0,$$

which will give an expression for c_{gk},

$$D_{\omega\omega} = -\int_{-H}^{H} 6k^2 \frac{N^2}{\omega^4}\phi^2 dy,$$

$$D_{\omega k} = \int_{-H}^{H} 4k \frac{N^2}{\omega^3} \phi^2 dy + \int_{-H}^{H} 4k^2 \frac{N^2}{\omega^3} \phi \phi_k dy ,$$

$$D_{k\omega} = \int_{-H}^{H} 4k \frac{N^2}{\omega^3} \phi^2 dy ,$$

$$D_{kk} = -\int_{-H}^{H} 2\left[\frac{N^2}{\omega^2} - 1\right] \phi^2 dy - \int_{-H}^{H} 4k \left[\frac{N^2}{\omega^2} - 1\right] \phi \phi_k dy .$$

The function ϕ_k satisfies the forced Taylor-Goldstein equation

$$\phi_{kyy} + k^2 \left[\frac{N^2}{\omega^2} - 1\right] \phi_k = -2k \left[\frac{N^2}{\omega^2} - 1\right] \phi + 2k^2 \frac{N^2}{\omega^3} c_g \phi, \quad -H < y < H , \quad \phi_k = 0 \text{ at } y = \pm H .$$

The compatibility condition yields c_g as above, but ϕ_k is not unique, as $\phi_k + C\phi$ is a solution for any constant *C*. However, the formula for c_{gk} is independent of *C*. Hence any possible solution for ϕ_k will be sufficient. These expressions can all be evaluated at the fixed wavenumber *k*.

4. Occurrence of internal rogue wave

A remarkable application of these exact linear eigenfunctions to the nonlinear dynamics of slowly varying wave packets will now be discussed. Following procedures outlined in the literature [10], a perturbation series is developed for the stream function Ψ using a small non-dimensional amplitude parameter (ε):

$\Psi = \Psi_0 + \varepsilon\Psi_1 + \varepsilon^2\Psi_2 + \varepsilon^3\Psi_3 + \ldots$

The leading order term will give a background shear flow while the first order term will yield the linear modal equation. The second harmonic, induced mean flow, and group

velocity for the wave packet can be obtained by collecting second order perturbation terms.

On applying the Fredholm Alternative Theorem at the level of the third order perturbation, a NLSE for a slowly varying envelope A can be derived:

$$iA_\tau + \beta A_{\xi\xi} + \gamma A^2 A^* = 0, \tag{16}$$

with $\tau = \varepsilon^2 t$, $\xi = \varepsilon(x - c_g t)$ being slow time and group velocity coordinate respectively, and * denotes the complex conjugate. The likelihood for the occurrence of internal rogue wave modes can then be assessed from the considerations of the second order dispersion term (measured by β), the cubic nonlinear term (γ) and the possible instability of plane waves. The sign of the product $\beta\gamma$ will dictate the dynamics, with envelope solitons, modulation instability and rogue wave only possible for $\beta\gamma > 0$ [10,11].

Two different models will be discussed, with no background current in the first one (the 'no shear' model), while the second one can allow for a linear shear flow. The formulations for calculating the second harmonic, induced mean motion, dispersion and cubic nonlinearity are developed earlier in the literature [10] (Appendix), with the calculations for the present situation being facilitated by the exact linear eigenfunctions obtained in Section 2.

4.1 'No shear' model

Three eigenfunctions ($\phi = \mathrm{sech}^2(ry) - \frac{2}{3}$, ϕ_a, and ϕ_b) are selected as the linear modes in the calculations in the nonlinear regime for the parameters of second order dispersion (β) and cubic nonlinearity (γ) for the 'no shear' model. The full formulation is given in the Appendix. Figure 5 and 6 show the second harmonic and induced mean flows associated with linear eigenfunctions of ϕ and ϕ_a.

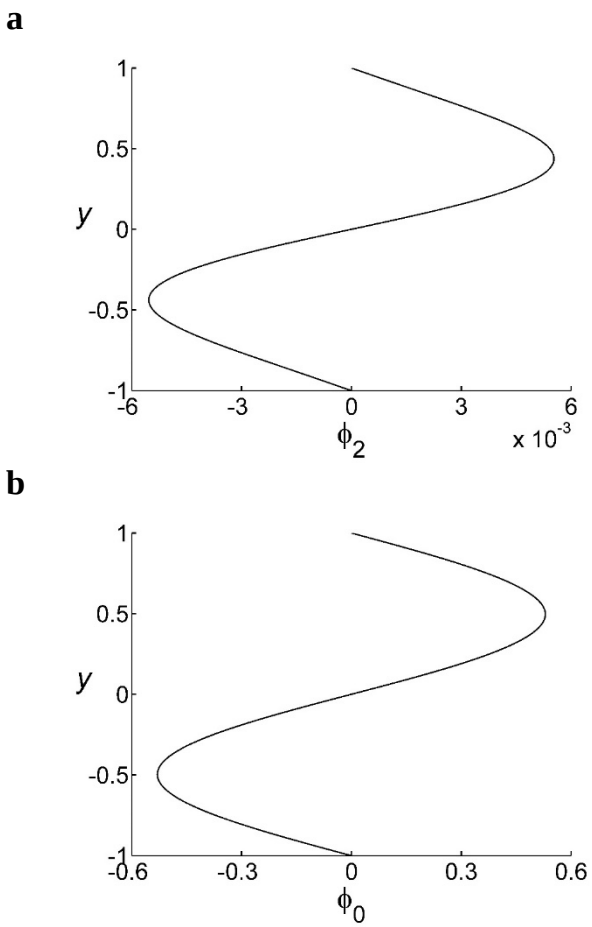

Fig. 5 (a) The profile of the second harmonic as a function of the vertical coordinate y, using the eigenfunction ϕ (Eq. (8)) as input, $-H < y < H$, $H = 1$; (b) Solution of the induced mean motion equation versus the vertical coordinate y using the eigenfunction ϕ (Eq. (8)) as input, $-H < y < H$, $H = 1$.

a

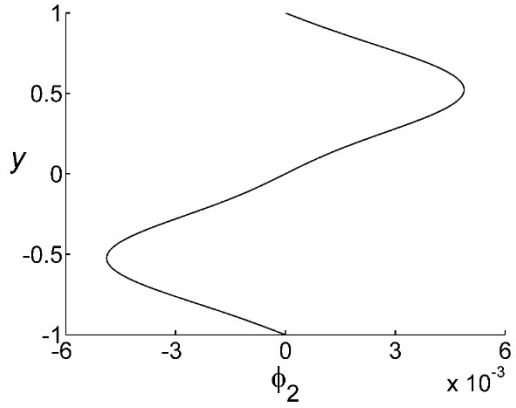

b

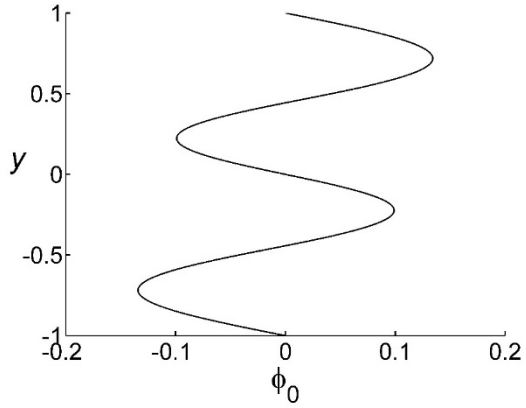

Fig. 6 (a) The profile of the second harmonic as a function of the vertical coordinate y, using the eigenfunction ϕ_a (Eq. (10)) as input, $-H < y < H$, $H = 1$; (b) Solution of the induced mean motion equation versus the vertical coordinate y, using the eigenfunction ϕ_a (Eq. (10)) as input, $-H < y < H$, $H = 1$.

Table 1 lists the coefficients of second order dispersion (β) and cubic nonlinearity (γ) for these three cases. All these three cases display negative values for the product $\beta\gamma$, which indicate that internal rogue waves are unlikely to occur.

Eigenfunction	β	γ	Sign of $\beta\gamma$
ϕ	0.1161	-0.9315	Negative
ϕ_a	0.0525	-1.2203	Negative
ϕ_b	0.0499	-0.4746	Negative

TABLE 1. Coefficients of dispersion and cubic nonlinearity for cases with eigenfunctions ϕ, ϕ_a and ϕ_b.

4.2 Linear shear model

Attempts to align the linear stability equation for stratified flows (Eq. (1)) with a linear Schrödinger equation with a 'sech^2' potential generally fail for an arbitrary shear profile $U(y)$. However, a special case of a linear shear will permit analytical progress, as the curvature of the profile (the vorticity gradient or theoretically the second derivative) will vanish. In that case, choosing a special buoyancy frequency $N^2/(U-c)^2 = \mathrm{sech}^2 ry$ will also allow exact solutions. More precisely, for the linear shear model ($U(y) = \lambda y$), the eigenfunction $\phi = \mathrm{sech}^2(ry) - \frac{2}{3}$ will be applied to elucidate the wave packet dynamics. The wavenumber k and the associated wave speed c will be evaluated using

mechanisms developed earlier. Figure 7 shows the solutions of the second harmonic and the induced mean motion equations with $k = 1$, $c = 2$ and $\lambda = 1$.

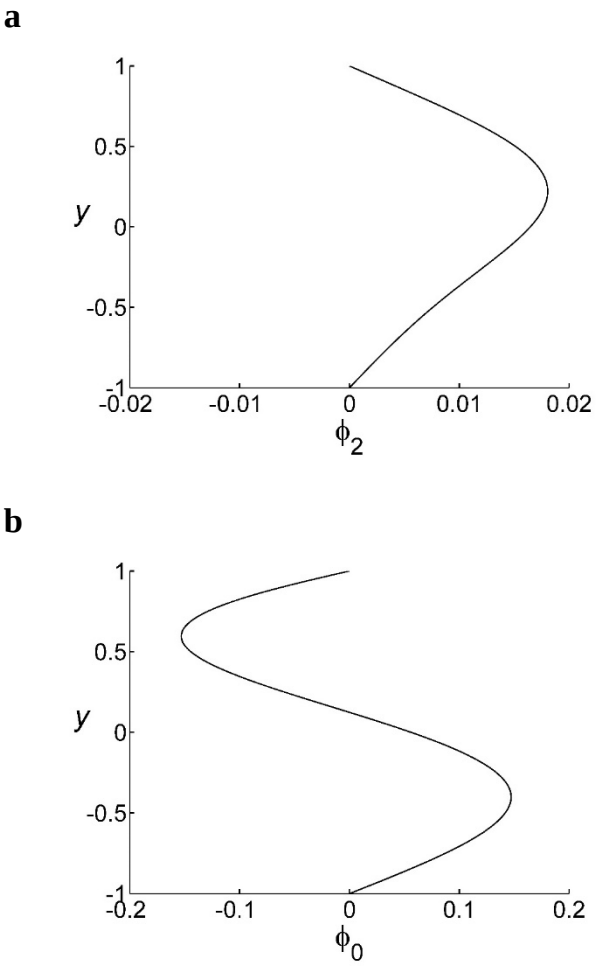

Fig. 7 (a) The profile of the second harmonic as a function of the vertical coordinate *y*, using the eigenfunction ϕ (Eq. (8)) as input, $k = 1$, $c = 2$, $\lambda = 1$, $-H < y < H$, $H = 1$;
(b) Solution of the induced mean motion equation versus the vertical coordinate *y*, using the eigenfunction ϕ (Eq. (8)) as input, $k = 1$, $c = 2$, $\lambda = 1$, $-H < y < H$, $H = 1$.

Table 2 lists the coefficients of quadratic dispersion (β) and cubic nonlinearity (γ) for a few selected examples. All these cases display positive values for the product $\beta\gamma$, which indicate internal rogue waves may likely occur.

Values of k and c	β	γ	Sign of $\beta\gamma$
$k = 1$, $c = 1.5$	0.2074	0.8942	Positive
$k = 1$, $c = 2$	0.2913	0.2963	Positive
$k = 1$, $c = 3$	0.4511	0.1523	Positive

TABLE 2. Coefficients of dispersion and cubic nonlinearity for cases with fixed k and varied c by starting with the linear eigenfunction ϕ (Eq. (8)).

5. A further example with constant buoyancy frequency

A simple example of constant buoyancy frequency permits explicit analytical expressions for the coefficients of the NLSE [10,11], and hence further insights on the formation and profile of rogue waves can be gained. In sharp contrast to surface waves where rogue waves exist only if the carrier wave packet is reasonably short ($kh > 1.363$), rogue waves in density stratified fluids can exist when the internal mode is much longer. More precisely, PB exists if a non-dimensional wavenumber is smaller than the critical threshold of $k_c = \sqrt{\sqrt[3]{4} - 1}\, m\pi$, where m is the mode number. Since the critical wavenumber k_c increases with m, the existence regime of rogue wave is extended for higher-order modes.

The wave profile and amplification ratio of a rogue wave are crucial elements in the dynamics. While the maximum amplitude of the PB is always three times the background amplitude, the spatial extent of the PB depends on both the coefficients of

dispersion and nonlinearity. More precisely, the PB with normalized background amplitude is given by [11],

$$A = \mathrm{e}^{\mathrm{i}\gamma\tau}\left\{1-\frac{2\left(1+2\gamma\tau\mathrm{i}\right)}{\gamma\left[\xi^2/\beta+2\gamma\tau^2+1/\left(2\gamma\right)\right]}\right\} \tag{17}$$

The maximum is located at the origin and the minima are attained at $\xi = \pm\sqrt{(3\beta)/(2\gamma)}$. In the case with a constant buoyancy frequency, the coefficients of dispersion (β) and nonlinearity (γ) are related by

$$\frac{\beta}{\gamma} = \frac{N^2}{4k^2}\left[\frac{4m^2\pi^2}{\left(m^2\pi^2+k^2\right)^3}-\frac{1}{m^4\pi^4}\right]. \tag{18}$$

Thus the PB occupies a larger spatial domain for a carrier wave with a smaller wavenumber. The PBs at various carrier wavenumbers are shown in Fig. 8 and the exact coefficients are documented in Table 3. In other words, the rogue wave arising from a carrier envelope packet with a larger wavenumber is steeper and more localized. Furthermore, for a fixed wavenumber, the PB corresponding to a high-order mode is steeper.

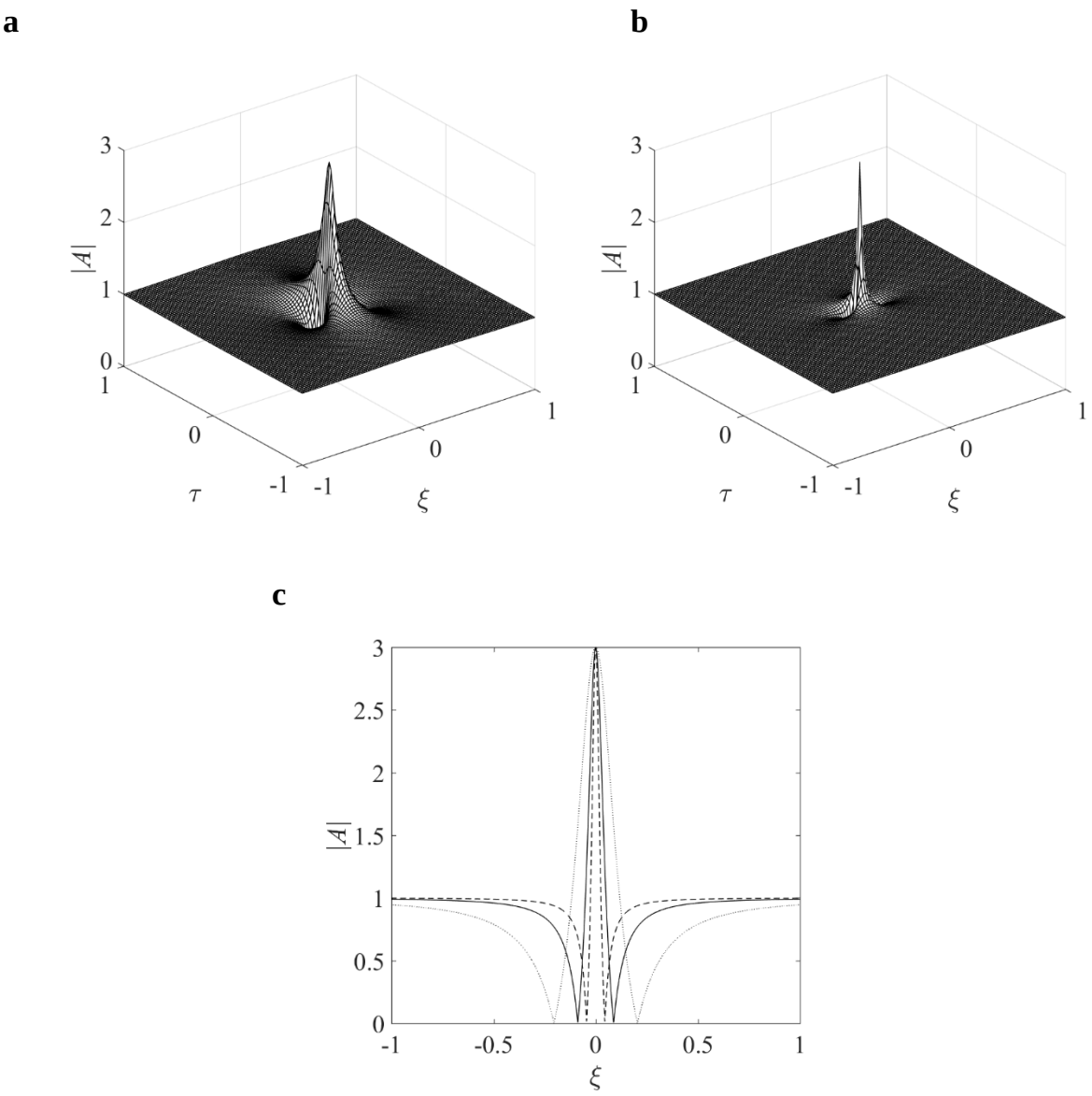

Fig. 8 The wave profile of the Peregrine breather of the NLSE versus space and time at $N = 1$, $m = 1$ and (a) $k = 1$; (b) $k = 1.5$. (c) The waveform at $\tau = 0$ with $N = 1$, $m = 1$: $k = 0.5$ (dotted line); $k = 1$ (solid line); $k = 1.5$ (dashed line).

k	β	γ	Sign of $\beta\gamma$
0.5	0.0227	0.817	Positive
1	0.038	7.42	Positive
1.5	0.0434	32.8	Positive

TABLE 3. Coefficients of dispersion and cubic nonlinearity for various wavenumbers at $N = 1$ and $m = 1$.

6. Discussion and conclusions

The main goal of this work is to elucidate theoretically the occurrence of internal rogue waves in density stratified flows. While internal rogue waves in long wave models have been studied in the literature [25], the present work focuses on unexpectedly large amplitude displacements arising from the propagation of internal wave packets. The first stage concentrates on calculating new exact solutions of the linear modal equations in a finite domain for realistic stratification profiles. The second step utilizes these exact solutions to facilitate the calculations of the second harmonic and the induced mean motion, leading to a nonlinear Schrödinger equation for a slowly varying wave packet. The balance of dispersion and nonlinearity would then determine the likelihood for the occurrence of rogue waves.

Firstly, exact solutions for the governing equation of the vertical spatial structure of linearized disturbances in a stratified flow are derived by comparison with solutions of coupled systems of nonlinear Schrödinger equations. The Boussinesq approximation is assumed, where the variation in the background density is neglected except in the

consideration of the buoyancy. Such coupled Schrödinger systems may display a remarkable feature, where the total induced mean flow (for hydrodynamic applications) or the total light beam intensity (for optical applications) can be expressed as the square of a hyperbolic secant, while each component consists of higher algebraic powers of hyperbolic functions.

As illustrative examples, coupled systems with four and five components are employed to calculate solutions for linearized stratified flows. One constraint on this technique is that these explicit expressions for linear modes are applicable only to specific values of the wavenumber. Nevertheless, a scheme to calculate the group velocity and the curvature of the dispersion relation (or the second derivative of the angular frequency with respect to the wavenumber) is presented. For an arbitrary wavenumber, a numerical solution of the linear modal equation may still be required, but the existence of such special analytical solutions will provide valuable insights about the flow structure.

Secondly, the nonlinear evolution of a wave packet is developed through calculations of the second harmonic, induced mean flow and eventually a canonical form of the nonlinear Schrödinger equation [3,10], facilitated by the exact expressions of the linear eigenfunctions. The likelihood for the occurrence of internal rogue wave modes can be assessed. For the cases where the buoyancy frequency has a hyperbolic secant profile, computations for the present family of modes typically yield cases of dispersion and nonlinearity of opposite signs, i.e. regimes devoid of rogue waves. However, in the

presence of a linear shear and a slightly modified density profile, dispersion and nonlinearity can share the same sign and rogue waves may thus exist in such regime. This feature highlights the importance of background current on the formation of rogue waves.

The existence of internal rogue waves is further examined for the special case where the buoyancy frequency is a constant. As opposed to surface rogue waves, internal rogue waves exist in the long wave regime where the wavenumber of the carrier envelope packet can be small. The threshold wavenumber varies among different internal modes. In terms of the wave form, the PB is steeper and more localized when the carrier envelope packet has a larger wavenumber. The methodology discussed in this work can be extended to systems with more components to obtain higher order solutions. Such higher order solutions and other density profiles will be tested in the future.

The present work thus hopefully serves as a remarkable application of nonlinear analysis to fluid mechanics and probably other real world applications. Firstly, known solutions of coupled nonlinear Schrödinger equations are utilized to establish special exact solutions of linear modes of stratified flows. Secondly, perturbation schemes in fluid mechanics confirm that a single component nonlinear Schrödinger equation will govern the evolution of a wave packet. On studying the nonlinear dynamics, one finally deduces the likelihood of the occurrence of internal rogue waves. In terms of further hydrodynamic applications, parameters for the buoyancy frequency can be chosen to model a realistic pycnocline density profile in the upper ocean. Further theoretical and computational efforts would then be fruitful.

Appendix

The nonlinear dynamics of a slowly varying wave packet will now be formulated, following similar schemes developed earlier in the literature [10]. For simplicity, we first discuss the case of no background shear ($U(y) = 0$) and the fluid is confined between $y = y_1$ and $y = y_2$. As discussed in the text, the buoyancy frequency will be either given by hyperbolic functions

$$N^2 = \alpha_1 \operatorname{sech}^2(ry) + \alpha_0,$$

or a constant value.

The second harmonic equation is given by (ϕ_1 being the linear mode)

$$\left(\frac{d^2}{dy^2} - 4k^2 + \frac{N^2}{c^2}\right)\phi_2 = \frac{1}{c^3}\left(N^2\right)_y \phi_1^2 .$$

The induced mean motion equation is governed by

$$\left(\frac{d^2}{dy^2} + \frac{N^2}{c_g^2}\right)\phi_0 = \frac{2}{c^3}\left(N^2\right)_y \phi_1^2 + \left(\frac{2}{c^3} - \frac{1}{c^2 c_g} - \frac{1}{c c_g^2}\right) N^2 \left(\phi_1^2\right)_y ,$$

where the group velocity is obtained by applying the Fredholm alternative condition,

$$c_g = c - \frac{\int_{y_1}^{y_2} \phi_1^2 dy}{\int_{y_1}^{y_2} \frac{kN^2}{\omega^3} \phi_1^2 dy} .$$

The coefficients of dispersion and cubic nonlinearity of Eq. (16) are given by

$$\beta = \frac{\int_{y_1}^{y_2}\left[1+\frac{N^2\left(c-c_g\right)\left(3c_g-c\right)}{k^2c^4}\right]\phi_1^2 dy + 2\int_{y_1}^{y_2}\left[-k+\frac{\left(c-c_g\right)N^2}{kc^3}\right]\phi_{11}\phi_1 dy}{2\int_{y_1}^{y_2}\frac{2kN^2}{\omega^3}\phi_1^2 dy},$$

$$\gamma = -\frac{\int_{y_1}^{y_2}\tilde{g}_1\phi_1 dy}{2\int_{y_1}^{y_2}\frac{k^2N^2}{\omega^3}\phi_1^2 dy},$$

where the function ϕ_{11} is determined from

$$\left(\frac{d^2}{dy^2}-k^2+\frac{N^2}{c^2}\right)\phi_{11} = 2\left[-k+\frac{\left(c-c_g\right)N^2}{kc^3}\right]\phi_1,$$

the other functions $\tilde{g}_1,\ f_0,\ g_0,\ f_2,\ g_2$ are listed as follows

$$\tilde{g}_1 = \frac{1}{c^2}\Bigg[2\phi_1'\left(cf_2-g_2\right)+\phi_1\left\{\left(g_0'-g_2'\right)-c\left(f_0'-f_2'\right)\right\}+2\phi_1\phi_2\frac{1}{c}\left(N^2\right)_y$$

$$+\frac{\phi_0\phi_1}{c_g}\left(\frac{c}{c_g}+1\right)\left(N^2\right)_y+\phi_1\phi_0'\left(\frac{1}{c_g}+\frac{c}{c_g^2}-\frac{2}{c}\right)N^2\Bigg],$$

$$f_0 = \frac{2}{c^3}\left(N^2\right)_y\phi_1^2+\left(\frac{2}{c^3}-\frac{1}{c^2c_g}-\frac{1}{cc_g^2}\right)N^2\left(\phi_1^2\right)_y,$$

$$g_0 = -\frac{1}{c^2}\left(N^2\right)_y\phi_1^2+\frac{1}{c^2}\left(\frac{c}{c_g}-1\right)N^2\left(\phi_1^2\right)_y,$$

$$f_2 = \frac{1}{c^3}\left(N^2\right)_y\phi_1^2,$$

$$g_2 = -\frac{1}{2c^2}\left(N^2\right)_y\phi_1^2.$$

If we allow for a linear shear ($U(y)=\lambda y$), the buoyancy frequency is given by

$$N^2=\left(\alpha_1\,\mathrm{sech}^2\left(ry\right)+\alpha_0\right)\left(\lambda y-c\right)^2.$$

The second harmonic equation for the linear shear model is then found by

$$\left[\frac{d^2}{dy^2}-4k^2+\frac{N^2}{\left(U-c\right)^2}\right]\phi_2=\frac{\phi_1^2}{2\left(U-c\right)^2}\left\{k\left(U-c\right)\left[-\frac{N^2}{k\left(U-c\right)^2}\right]_y-\left(\frac{N^2}{U-c}\right)_y\right\}.$$

The induced mean motion for the linear shear model is determined by

$$\left[\frac{d^2}{dy^2}+\frac{N^2}{\left(U-c_g\right)^2}\right]\phi_0=\phi_1^2\frac{1}{U-c_g}\left\{\left[-\frac{N^2\left(c+U-2c_g\right)}{\left(U-c\right)^3}\right]_y-\frac{1}{\left(U-c_g\right)}\left[\frac{N^2\left(U-c_g\right)}{\left(U-c\right)^2}\right]_y\right\}$$

$$-\left(\phi_1^2\right)_y\frac{\left(c-c_g\right)N^2}{\left(U-c\right)^2\left(U-c_g\right)}\left[\frac{2}{\left(U-c\right)}+\frac{1}{\left(U-c_g\right)}\right].$$

where the group velocity is obtained by

$$c_g=c-\frac{\int_{y_1}^{y_2}\phi_1^2dy}{\int_{y_1}^{y_2}\frac{N^2}{k^2\left(c-U\right)^3}\phi_1^2dy}.$$

The coefficients of quadratic dispersion and cubic nonlinearity of Eq. (16) are given by

$$\beta=-\frac{\int_{y_1}^{y_2}\left[1+\frac{N^2\left(c-c_g\right)\left(3c_g-2U-c\right)}{k^2\left(U-c\right)^4}\right]\phi_1^2dy-2\int_{y_1}^{y_2}\left[k+\frac{\left(c-c_g\right)N^2}{k\left(U-c\right)^3}\right]\phi_{11}\phi_1dy}{4\int_{y_1}^{y_2}\frac{N^2}{k^2\left(U-c\right)^3}\phi_1^2dy},$$

$$\gamma = \frac{\int_{y_1}^{y_2} \tilde{g}_1 \phi_1 dy}{2\int_{y_1}^{y_2} \frac{N^2}{k(U-c)^3} \phi_1^2 dy},$$

where the function ϕ_{11} is solved by this equation

$$\left[\frac{d^2}{dy^2} - k^2 + \frac{N^2}{(U-c)^2}\right]\phi_{11} = -2\left[k + \frac{(c-c_g)N^2}{k(U-c)^3}\right]\phi_1 .$$

The other functions $\tilde{g}_1,\ f_0,\ g_0,\ f_2,\ g_2$ are listed as follows

$$\tilde{g}_1 = \frac{1}{(U-c)^2}\left\{\frac{d\phi_1}{dy}\left[-2(U-c) f_2 - 2g_2\right] + \phi_1\left[(g_0' - g_2') + (U-c)(f_0' - f_2')\right]\right.$$

$$+\phi_1\phi_2\left[(U-c)\left\{-\frac{N^2}{(U-c)^2}\right\}_y - \left(\frac{N^2}{U-c}\right)_y\right] + \phi_0\phi_1\left[(U-c)\left\{-\frac{N^2}{(U-c_g)^2}\right\}_y - \left(\frac{N^2}{U-c_g}\right)_y\right]$$

$$\left.+\phi_1\frac{d\psi_0}{dy}\left[\frac{2N^2}{U-c} - \frac{(U-c)N^2}{(U-c_g)^2} - \frac{N^2}{U-c_g}\right]\right\},$$

$$f_0 = \phi_1^2\frac{1}{U-c_g}\left\{\left[-\frac{N^2(c+U-2c_g)}{(U-c)^3}\right]_y - \frac{1}{(U-c_g)}\left[\frac{N^2(U-c_g)}{(U-c)^2}\right]_y\right\}$$

$$-\left(\phi_1^2\right)_y\frac{(c-c_g)N^2}{(U-c)^2(U-c_g)}\left[\frac{2}{(U-c)} + \frac{1}{(U-c_g)}\right],$$

$$g_0 = -\frac{(c-c_g)N^2}{(U-c_g)(U-c)^2}\left(\phi_1^2\right)_y - \frac{1}{U-c_g}\left[\frac{(U-c_g)N^2}{(U-c)^2}\right]_y \phi_1^2,$$

$$f_2 = \frac{\phi_1^2}{2(U-c)^2}\left\{k(U-c)\left[-\frac{N^2}{k(U-c)^2}\right]_y - \left(\frac{N^2}{U-c}\right)_y\right\},$$

$$g_2 = -\frac{k}{2(U-c)}\left[\frac{N^2}{k(U-c)}\right]_y \phi_1^2.$$

Acknowledgement

Partial financial support has been provided by the Research Grants Council contract HKU 17200815. RHJG was supported by the Leverhulme Trust through the award of a Leverhulme Emeritus Fellowship. This research is conducted using the University of Hong Kong Information Technology Services research computing facilities that are supported in part by the Hong Kong University Grants Committee Special Equipment Grant (SEG HKU09).

References

[1] K.R. Helfrich, W.K. Melville, Long nonlinear internal waves, Ann. Rev. Fluid Mech. 38 (2006) 395–425.

[2] C. Staquet, J. Sommeria, Internal gravity waves: From instabilities to turbulence, Ann. Rev. Fluid Mech. 34 (2002) 559–593.

[3] A.D.D. Craik, Wave Interactions and Fluid Flows, Cambridge University Press, Cambridge, 1984.

[4] H.E. Huppert, On Howard's technique for perturbing neutral solutions of Taylor-Goldstein equation, J. Fluid. Mech. 57 (1973) 361–368.

[5] R. Barros, W. Choi, Elementary stratified flows with stability at low Richardson number, Phys. Fluids 26 (2014) 124107.

[6] J. Lekner, Reflectionless eigenstates of the sech^2 potential, Am. J. Phys. 75 (2007) 1151–1157.

[7] R. Ivanov, Hamiltonian model for coupled surface and internal waves in the presence of currents, Nonlinear Anal. Real World Appl. 34 (2017) 316–334.

[8] O. Christov, Non-integrability of the Karabut system, Nonlinear Anal. Real World Appl. 32 (2016) 91–97.

[9] H. C. Hsu, C. I. Martin, Azimuthal equatorial capillary-gravity flows in spherical coordinates, Nonlinear Anal. Real World Appl. 36 (2017) 278–286.

[10] A.K. Liu, D.J. Benney, The evolution of nonlinear wave trains in stratified shear flows, Stud. Appl. Math. 64 (1981) 247–269.

[11] D.H. Peregrine, Water waves, nonlinear Schrodinger equations and their solutions, J. Aust. Math. Soc. B. 25 (1983) 16–43.

[12] K. Dysthe, H.E. Krogstad, P. Müller, Oceanic rogue waves, Ann. Rev. Fluid Mech. 40 (2008) 287–310.

[13] A. Chabchoub, N. Hoffmann, M. Onorato, N. Akhmediev, Super rogue waves: observation of a higher-order breather in water waves, Phys. Rev. X 2 (2012) 011015.

[14] L. Shemer, L. Alperovich, Peregrine breather revisited, Phys. Fluids 25 (2013) 051701.

[15] A. Davey, K. Stewartson, On three-dimensional packets of surface waves, Proc. R. Soc. Lond. A. 338 (1974) 101–110.

[16] M.J. Ablowitz, H. Segur, On the evolution of packets of water waves, J. Fluid Mech. 92 (1979) 691–715.

[17] G. Mu, Z. Qin, Two spatial dimensional N-rogue waves and their dynamics in Mel'nikov equation, Nonlinear Anal. Real World Appl. 18 (2014) 1–13.

[18] G. Mu, Z. Qin, Dynamic patterns of high-order rogue waves for Sasa-Satsuma equation, Nonlinear Anal. Real World Appl. 31 (2016) 179–209.

[19] L. Ling, B.F. Feng, Z. Zhu, General soliton solutions to a coupled Fokas-Lenells equation, Nonlinear Anal. Real World Appl. 40 (2018) 185–214.

[20] F.T. Hioe, Solitary waves for two and three coupled nonlinear Schrödinger equations, Phys. Rev. E 58 (1998) 6700–6707.

[21] F.T. Hioe, T.S. Salter, Special set and solutions of coupled nonlinear Schrödinger equations, J. Phys. A 35 (2002) 8913–8928.

[22] K.W. Chow, Periodic solutions for a system of four coupled nonlinear Schrödinger equations, Phys. Lett. A 285 (2001) 319–326.

[23] K.W. Chow, D.W.C. Lai, Periodic solutions for systems of coupled nonlinear Schrödinger equations with five and six components, Phys. Rev. E 65 (2002) 026613.

[24] Y.S. Kivshar, G.P. Agrawal, Optical Solitons: From Fibers to Photonic Crystals, Academic Press, San Diego, 2003.

[25] R. Grimshaw, E. Pelinovsky, T. Taipova, A. Sergeeva, Rogue internal waves in the ocean: Long wave model, Eur. Phys. J.-Spec. Top. 185 (2010) 195–208.